JCTC Journal of Chemical Theory and Computation

ARTICLE

pubs.acs.org/JCTC

Theoretical Investigations on the Photoinduced Phase Transition Mechanism of Tetrathiafulvalene-*p*-chloranil

Yutaka Nakatsuka,[†,‡] Takao Tsuneda,[*,†,‡] Takeshi Sato,[§] and Kimihiko Hirao[†,‡]

[†]Advanced Science Institute, RIKEN 2-1, Hirosawa, Wako, Saitama 351-0198, Japan

[‡]CREST, Japan Science and Technology Agency, Saitama 332-0012, Japan

[§]Photon Science Center of the University of Tokyo, Tokyo 113-8656, Japan

ABSTRACT: The photoinduced phase transition (PIPT) mechanism of tetrathiafulvalene-*p*-chloranil (TTF-CA) molecular crystal was theoretically investigated using the long-range corrected time-dependent density functional theory (LC-TDDFT) combined with a local response dispersion (LRD) method, which enables us to quantitatively reproduce charge transfer (CT) excitations of van der Waals clusters. By calculating the excitation spectrum and potential energy surface, we found that the PIPT of TTF-CA crystal may proceed through the angle change of the molecular planes. We also found that the CT excitation of one TTF-CA pair helps other neighboring TTF-CA pairs to become excited. Consequently, we theoretically proposed the initial structural change in the neutral-to-ionic PIPT of TTF-CA crystal, which is consistent with experiments.

I. INTRODUCTION

For the last 3 decades, the neutral−ionic phase transitions of alternatively stacked molecular crystals, which consist of electron donor (D) and acceptor (A) molecules, have been extensively studied due to their potentials for new materials and their unique physical phenomena. These phase transitions have been known to be induced by pressure and temperature. Recently, some phase transitions have also been found to be induced by photoirradiation. These photoinduced phase transitions (PIPT) can be distinguished in that a local change in electric structure leads to a macroscopic change in the crystal structure. The PIPT has been attracting interest as a new physical phenomenon and as a route to promising photoswitching devices.

Tetrathiafulvalene-*p*-chloranil (TTF-CA) molecular crystal, which consists of tetrathiafulvalene (TTF) donor and *p*-chloranil (CA) acceptor molecules, is a typical PIPT material. After Mayerle et al.[1] had observed a mixed-stack structure of TTF-CA crystal, Torrance et al. found that TTF-CA crystal is on the boundary of ionic (I) and neutral (N) states and undergoes pressure-induced[2] and temperature-induced[3] phase transitions: in high temperature or low pressure, TTF-CA crystal is in the N state, where TTF and CA molecules are alternatively stacked along the *a* direction (Figure 1) with equivalent distances. On the other hand, in low temperature or high pressure, TTF-CA crystal is in the I state, where TTF and CA molecules are dimerized. The crystal structures and charge-transfer rates have been determined for each state by neutron diffraction[4] and molecular vibration analyses.[5] Koshihara et al.[6] found that at around the critical temperature (84 K), laser irradiation induces the phase transitions from I to N and from N to I states. To figure out this PIPT mechanism, many studies have been reported. The initial mechanism of the I-to-N PIPT has been especially eagerly studied with picosecond[7,8] and femtosecond[9,10] time-resolved spectroscopies. The N-to-I PIPT was also investigated to confirm that no phase transition is induced by temperature increase via the laser irradiation.[11] Okamoto et al.[12] investigated the dynamics of both

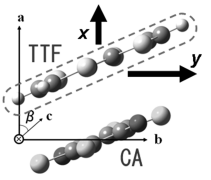

Figure 1. The structure of TTF-CA monomer and the orientations of the coordinates varied.

I-to-N and N-to-I PIPT with a femtosecond time-resolved spectroscopy and found that in the N-to-I PIPT, the one-dimensional domain in the I state is formed within 200 fs by the laser irradiation. These studies showed that the mechanisms of I-to-N and N-to-I PIPT significantly differ. The most significant difference is the threshold behavior only observed in the I-to-N PIPT.[9] The study of dynamics of N-to-I PIPT has shown the existence of ultrafast generation of an intermediate state, where the electronic and lattice changes are strongly coupled.[12−16]

In theoretical studies, this phase transition has been investigated on simple models and model Hamiltonians with empirical parameters. For the pressure-induced and temperature-induced phase transitions, Metzger and Torrance[17] showed in semiempirical calculations that the electron transfer energy from donor to acceptor and the Madelung energy play essential roles in the N-to-I phase transition. The importance of the Madelung energy was also stressed on the model calculation with the Hartree−Fock charge distribution by Kawamoto et al.[18] Soos et al.[19] applied a diagrammatic valence bond theory to investigate the CT absorption spectrum. For the PIPT, Nagaosa and Ogawa[20] outlined a mechanism in the framework of the kinetic Ising model. Huai et al.[21] calculated the adiabatic relaxation path on the extended Hubbard model and suggested the critical domain size in the I-to-N PIPT.

Received: December 12, 2010
Published: June 02, 2011

Yonemitsu also explained the I-to-N and N-to-I phase transitions on the extended Hubbard model.[22−24] Further theoretical works with model Hamiltonians can be found in the review by Yonemitsu and Nasu[25] and references therein. These model Hamiltonian calculations have qualitatively discussed the nature of PIPT. As for the quantitative discussion, a few works have been performed on density functional theory (DFT). However, past DFT calculations[26−29] have lacked both van der Waals (vdW) correlation and long-range exchange interactions. Molecular crystals are known to consist of weak vdW interactions. Also, long-range exchange interactions are reportedly required to give accurate CT excitations, while CT excitations have been suggested to be the main intermediates in the PIPT. Despite these inevitabilities, vdW correlation and long-range exchange have been neglected in molecular crystal calculations mainly due to their high computational cost.

In this study, we use long-range corrected time-dependent DFT (LC-TDDFT)[30] combined with the local response dispersion (LRD) correction to reveal the N-to-I PIPT mechanism of TTF-CA crystal. It has been suggested that the long-range correction (LC) scheme[31] enables TDDFT to quantitatively calculate CT excitation energies and oscillator strengths, which have been significantly underestimated in conventional TDDFT calculations,[32] without increasing the computational cost. It has also been reported that the LRD correction[33] gives accurate vdW bonds with no empirical parametrization by combining with the LC scheme.[34] We assume that electron itinerancy affects the N-to-I PIPT only through the background charges, because we suppose that in contrast to metals and semiconductors, TTF-CA crystal has only a very narrow conduction band attributing to the lowest CT excitation and therefore itinerant electrons may not directly affect the electronic states. We suppose that the initial N-to-I process of this PIPT can be treated by the single reference method because the starting point (N state) can be well-described with a single reference method. In this study, we focus on the N-to-I PIPT, because as mentioned later, we found that the I phase seems to have a multiconfigurational wave function, which is not appropriately calculated by DFT. As far as we know, this is the first calculation taking into account both long-range exchange and vdW correlation in TDDFT calculations of molecular crystals.

II. COMPUTATIONAL DETAILS

All DFT and TDDFT calculations have been carried out on the generalized Kohn−Sham method[35] using the LC scheme applied to Becke 1988 exchange[36] + one-parameter progressive correlation functional[37] (LC-BOP). In the LC scheme, the only parameter, μ, is set as $\mu = 0.33$, which is the optimum value in excited state calculations.[30] As the basis set, we use the 6-31G(d) basis functions.[38−40] The vdW correlation energy is calculated by the LRD method.[33] In LRD calculations, we assumed that the vdW correlation energies of the CT state, $\Delta E_{\mathrm{LRD}}^{\mathrm{CT}}$, are well-approximated by those of the triplet state, $\Delta E_{\mathrm{LRD}}^{\mathrm{triplet}}$, at the same geometries, i.e.,

$$E_{\mathrm{total}}^{\mathrm{GS}} = E_{\mathrm{LC\text{-}BOP}}^{\mathrm{GS}} + \Delta E_{\mathrm{LRD}}^{\mathrm{GS}} \quad (1)$$

$$E_{\mathrm{total}}^{\mathrm{CT}} = E_{\mathrm{LC\text{-}BOP}}^{\mathrm{CT}} + \Delta E_{\mathrm{LRD}}^{\mathrm{triplet}} \quad (2)$$

This is because the triplet state has similar electron distribution to the CT state and the vdW energy of the LRD method does not depend on the spin. All the calculations are carried out using the development version of Gaussian 03 program.[41] The molecular structure has been taken from the experimental neutron diffraction data at 90 K.[4] For simplicity, the term "TTF-CA pair" is used to represent the pair of TTF and CA molecules stacked in the *a* direction (Figure 1).

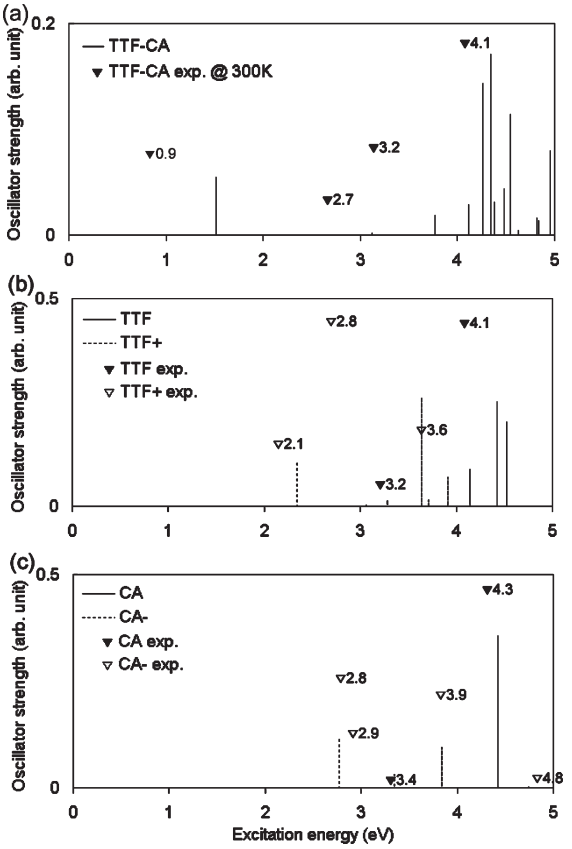

Figure 2. The calculated excitation spectrum of (a) TTF-CA monomer for the experimental structure at 90 K, (b) TTF molecule and TTF^+ cation, and (c) CA molecule and CA^- anion. Experimental peaks of TTF-CA crystal at 300 K.[3] TTF, TTF^+,[42] CA, and CA^-[43] are also shown. The 6-311++G** basis set is used.

The position of the TTF molecule is varied in the *a* and *b* directions from the original position at the experimental structure, while the intramolecular structures of TTF and CA molecules are fixed at the experimental structures at 90 K.

The excitation spectrum of TTF-CA crystal is calculated using the embedded model of one TTF-CA pair in background point charges which represent surrounding TTF-CA pairs. The Peierls instability is taken into account only for the electrostatic effect by imposing sequential background point charges representing the Peierls-distorted charge distribution. The point charges are positioned on the atoms of the surrounding TTF-CA pairs on both sides of the *a* axis. The structures of neighboring pairs are set to be always parallel to the central TTF-CA pair. To fix the lattice constant, the distances between two TTF molecules are unchanged. The magnitudes of point charges are determined by the Mulliken charges of the CT state of the central TTF-CA pair. In this study, we use only the CT state charges, because we found that the charges of the ground state negligibly affect the excitation spectrum of a TTF-CA pair.

III. RESULTS AND DISCUSSION

TTF-CA Monomer. Before discussing the photoinduced phase transition mechanism of TTF-CA molecular crystal, let us

consider the electronic structure of TTF-CA monomer to make clear the molecular nature of this system. This may also be of help in examining our method for reproducing the excitation energies of such vdW complexes. Experimentally, the photoabsorption spectra of TTF-CA crystal have been observed in film and powder forms at 11 and 300 K.[3]

Figure 2a shows the calculated excitation spectrum of TTF-CA monomer for the experimental optimal structure at 90 K. In the figure, the lowest excitation at 1.52 eV corresponds to the CT excitation from HOMO to LUMO, which are both localized in TTF and CA, respectively, as shown in Figure 3.

Note that this CT excitation energy is higher than the lowest peak energy of TTF-CA crystal, 0.9 eV, in the experimental absorption spectrum at 300 K.[3] In addition, the ionicities of the ground and excited states—calculated as the sum of Mulliken charges—are almost zero and unity, respectively. Later, we will show that this discrepancy can be explained with the electrostatic effect from the surrounding TTF-CA units. The figure also shows strong peaks for 4−5 eV, which are also observed in the experimental absorption spectrum. These peaks correspond to the excitations of constituent TTF and CA molecules, in agreement with the experimental assignments. Figure 2b,c illustrates the calculated excited spectra of TTF, TTF^+, CA, and CA^-. In these TDDFT calculations, the larger 6-311++G** basis set[44−46] has been used because the higher energy excitations (over 4.0 eV) of TTF molecule was not sufficiently reproduced with the 6-31G(d) basis set. These figures indicate that as the experiment assigned, the peaks at 2.3 and 2.9 eV in the absorption spectrum of TTF-CA crystal at 11 K[3] correspond to the lowest excitations of TTF^+ and CA^-, respectively. Experimental peak of TTF, TTF^+, CA, and CA^- in CH_3CN can be found in the literature.[42,43] The accuracies in the excitation spectra support the reliability of the present method in excited state calculations of vdW complexes. In the following calculations, smaller 6-31G(d) basis set is used because the lowest CT excitation energy, which plays the main role in PIPT, was not significantly affected by improving basis set: the calculated CT excitation energies were 1.517 and 1.613 eV with the 6-311++G** and 6-31G(d) basis sets, respectively.

Next, we calculated the potential energy surfaces of TTF-CA monomer to clarify the structural dependence. The structures are varied for x and y coordinates given in Figure 1. Parts a and b of Figure 4 show the calculated potential energy surfaces of TTF-CA monomer for the ground and lowest CT excited states, respectively.

As shown in Figure 4a, the ground state has double minima: one is near the experimental structure (G), in which the distance between TTF and CA centers is 3.57 Å, and the other is symmetrical to this G structure (G′). These are slipped structures. Between G and G′ structures, the ground state has a low barrier with 0.11 eV. In contrast, Figure 4b shows that the lowest CT state has a single minimum at around the top of the barrier, which corresponds to a symmetrical structure and has 3.39 Å for the distance between TTF and CA centers. The G and E structures are illustrated in Figure 5. The low barrier between the G and G′ structures in the ground state shows that one TTF-CA pair can easily oscillate between two stable structures by the thermal fluctuations in the high-temperature. However, there are no experimental results concerning the dynamic slipping motion. This could be explained by considering a steric hindrance. Since only one TTF-CA pair is explicitly calculated in this study, we have considered no steric hindrance from neighboring TTF-CA pairs. When we explicitly calculated two TTF-CA pairs, we found that the steric hindrance between two pairs is affected by the interrelation of their structures. The steric hindrance is small if two pairs move in a coherent motion (the structures of the neighboring pairs are always parallel to the central pair). On the other hand, we found that when two pairs move randomly between G and G′ structures, the steric effect is much larger than the calculated energy barrier in one pair model and both pairs tend to stay in the energetically optimal G structure. Thus,

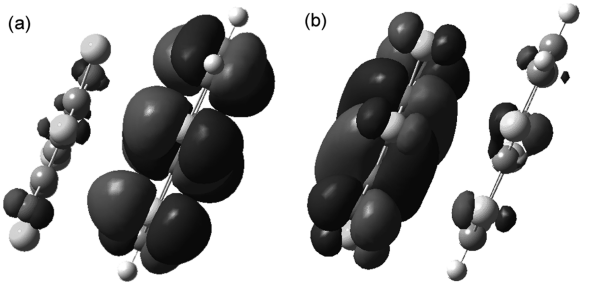

Figure 3. (a) HOMO and (b) LUMO of TTF-CA monomer.

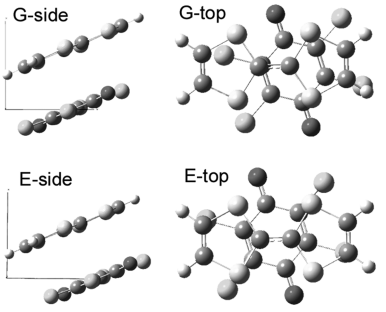

Figure 5. The side and overhead views of the G and E structures of TTF-CA monomer.

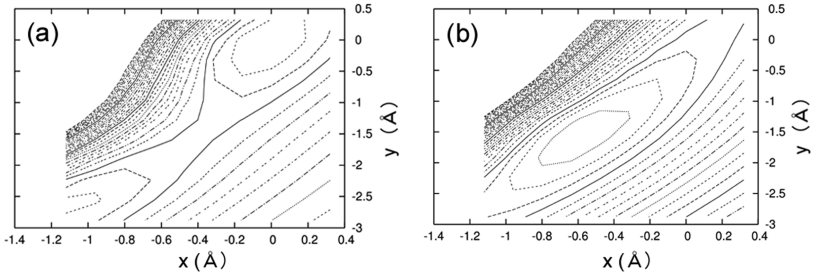

Figure 4. Calculated potential energy surfaces of TTF-CA monomer for (a) the ground state and (b) the lowest CT state. (Isovalues = 0.05 eV).

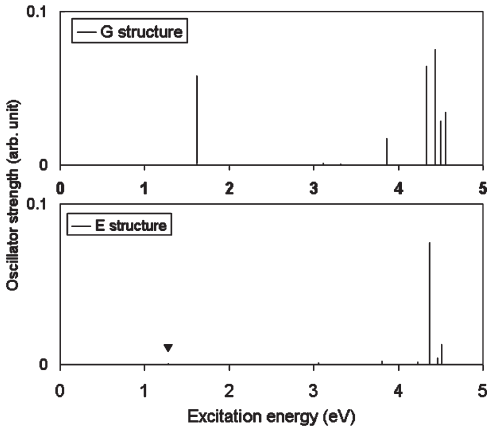

Figure 6. The calculated excitation spectra of TTF-CA monomer in the G and E structures. The black triangle indicates the position of CT excitation energy in the E structure.

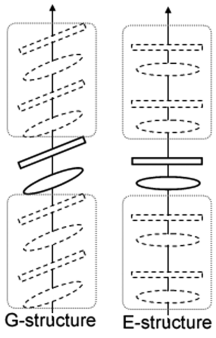

Figure 7. A possible structural change in TTF-CA crystal. Neighboring TTF-CA pairs illustrated with dotted lines are modeled with point charges in the present calculations.

we suppose that the double-well character of the ground state could not be observed unless the coherent motion of many TTF-CA pairs is realized. According to this supposition, we guess that the coherent motion of many TTF-CA pairs would be unlikely to occur in the high-temperature N phase. Note that in the case of TTF-CA crystal, the interstack hydrogen bonds—which are ignored in this study—would make the double-well potential energy surface of the ground state somewhat asymmetric. However, an experimental reflection spectrum study[12] showed that metastatic phases grow in the *a* direction in the early stage of the PIPT, indicating that the interstack bonds may not play a main role in the initial stage of the PIPT. The overhead views of these structures show that the TTF and CA centers overlap with each other in the E structure.

Figure 6 displays the calculated excitation spectra of TTF-CA monomer for the G and E structures. This figure indicates that the oscillator strength of the CT excitation drastically decreases between the G and E structures. The small oscillator strength is expected to make the de-excitation unlikely and to produce a long-lived CT excitation.

TTF-CA Molecular Crystal. On the basis of the above-mentioned features of TTF-CA monomer, let us consider the initial dynamics of PIPT in TTF-CA crystal. Considering that the optimal structure is transformed from the slipped G structure of the ground state to the symmetrical structure of the lowest CT state, we suppose that photoabsorption may change the crystal

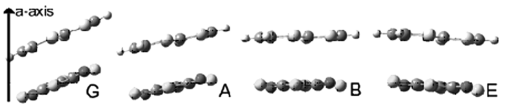

Figure 8. Calculated structures of the TTF-CA unit: G, $x = -0.04$, $y = -0.04$; A, $x = -0.16$, $y = -0.64$; B, $x = -0.32$, $y = -1.28$; E, $x = -0.58$, $y = -1.52$. Coordinates x and y are given in Figure 1.

structure for the molecular plane angle to the stacking axis, as shown in Figure 7.

This angle change is also expected to trigger a wide range of molecular plane angle shifts in neighboring TTF-CA pairs. To examine the effect of the angle change, excitation spectra are calculated for the G and E structures and two other structures between them (A and B) given in Figure 8.

The surrounding excited TTF-CA pairs—20 pairs on each side of the *a* direction—are taken into account as the point charge. Figure 9 shows the excitation spectra of (a) TTF-CA monomer and (b) TTF-CA crystal for these structures.

As shown in the figure, the structural change from G to E monotonically decreases the lowest CT excitation energy and the corresponding oscillator strength. However, for TTF-CA monomer, the structural effect is too small to make the CT excitation energy close to the experimental value (0.9 eV). On the other hand, in the crystal model with surrounding charges, the CT excitation energy is remarkably decreased even with a few pairs of the point charges of TTF-CA pairs. The CT excitation energies for the G and E structures are plotted in Figure 10 as a function of the number of surrounding point charges of TTF-CA pairs.

The structural change in TTF-CA crystal from G to E drastically decreases the CT excitation energy and makes it very close to the experimental value for the A structure. Simultaneously, the oscillator strength is decreased by the structural change from G to E to give a very small value for the E structure. This may cause the long-lived CT excitation mentioned above. The Mulliken charge ionicity of the ground state in G structure is 0.23, which is close to 0.3, the experimental estimation of ionicity in the N phase. On the other hand, the ground state ionicity at the E structure (0.02) is much lower than that of the I phase (0.6−0.7).[47,48] This ionicity implies that the E structure does not correspond to the I phase. Notice that the experimental structure of the I phase at low temperature is not so different from that of the N phase.[4] We therefore suppose that the I phase also has a structure close to the G structure in the direction of the slipping mode with the dimerization, although the ionicity cannot be reproduced, probably due to the neglect of explicit TTF-CA pairs.

On the calculated results, let us consider the mechanism of the N-to-I PIPT. First, we would like to emphasize that our model using one TTF-CA model with surrounding point charges quantitatively reproduces the experimental excitation spectra of TTF-CA crystal as mentioned above. We also found that this model gives the ground state optimum structure and ionicity close to those of the N phase. These results may indicate that our model is appropriate to discuss, at least the initial process of the N-to-I PIPT process of TTF-CA crystal. On the basis of the results, we propose that the initial N-to-I PIPT proceeds through the slipping motion from the G to E structures. A recent time-resolved Laue crystallography study has shown the fast formation of an intermediate structure after photoabsorption.[14] This experimental result is consistent with the present result showing

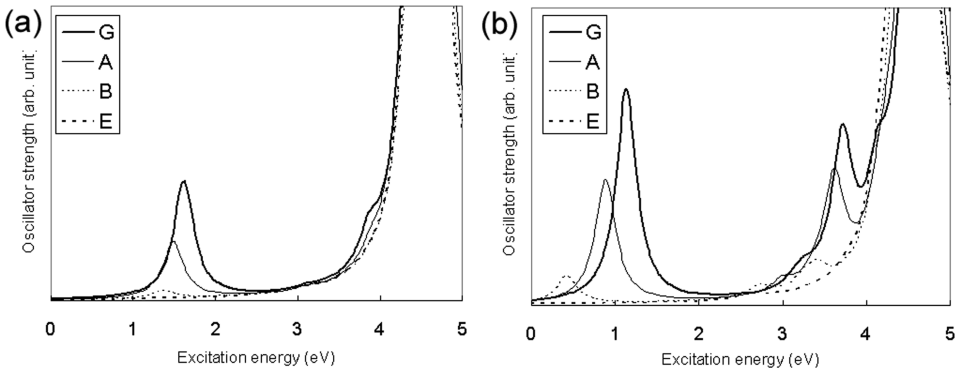

Figure 9. Calculated excitation spectra of (a) TTF-CA monomer and (b) TTF-CA crystal.

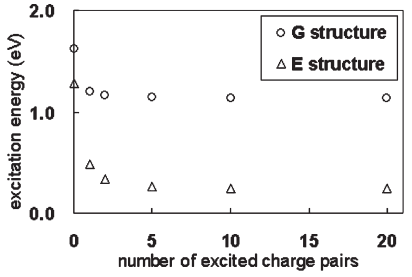

Figure 10. Calculated excitation energies of TTF-CA pair at the G and E structures with respect to the number of background excited TTF-CA pairs.

that TTF-CA transforms to the E structure, which is the optimum structure of the CT state. This would be experimentally confirmed because this transformation immediately affects the inversion symmetry of TTF-CA crystal due to the short distance between TTF and CA at the E structure, while it does not directly affect other diffraction peaks due to the local structural change. On the basis of the calculated result, we suppose that the E structure corresponds to the intermediate structure of the N-to-I PIPT observed in the time-resolved Laue crystallography.

For further analysis of the PIPT, let us consider the nature of the I phase and its generation process. Following previous experimental and theoretical studies, we assume that the I phase would be the long sequence of coherently polarized TTF-CA pairs, which is stabilized by Madelung and Peierls effects. Conceptual potential energy surfaces are illustrated in Figure 11. On the present model using one TTF-CA pair (Figure.11a), the I phase is always less stable than the N phase for any structure. Assuming that a bunch of neighboring TTF-CA pairs move in coherent motion (Figure.11b), we suppose that the I phase would get more stable than the N phase at around the G structure because of the Madelung and Peierls effects. On the other hand, we presume that at around the E structure, the N phase would be more stable than the I phase. This is because the TTF-CA pair is supposed to be less stabilized at the E structure by the background charges than that at the G structure due to the small ionicity. Therefore, we expect that the potential energy surfaces of the I and N phases intersect with each other at between the G and E structures. Although the I phase could not be obtained on the present model, the generation of the I phase could be explained on the structural and electronic changes in the present calculations.

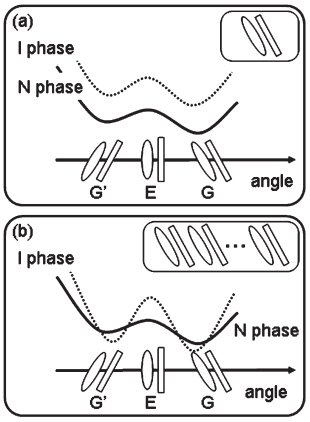

Figure 11. Conceptual potential energy curves of I and N phases along the slipping mode of TTF-CA pair (a) for one TTF-CA pair and (b) for a considerable number of coherent TTF-CA pairs.

With the above discussions, we propose that the N-to-I PIPT proceeds at the initial stage as follows (Figure 12):

(i) The ground state of TTF-CA cluster has a shallow potential energy surface with double minima (G and G′ structures). Due to the steric effect, TTF-CA pairs remain in the vicinity of one side (G) structure. The thermal lattice vibration is also centered at the G structure even at high temperature.

(ii) At high temperature, a TTF-CA pair in the crystal is photoexcited to the lowest CT state by laser irradiation at a certain point on the PES. The CT excitation induces the drastic change in the charge distribution and consequently triggers the excitations of neighboring TTF-CA pairs.

(iii) The sequence of excited TTF-CA pairs is then transformed into the E structure because the CT state has a single minimum at the E structure on the potential energy surface. The CT state may be long-lived due to the small oscillator strength at the E structure. Since the intermolecular distance is shortened from G to E structures, TTF-CA pairs are dimerized to break the inversion symmetry after the CT excitation. Then, PIPT may proceed through the lattice oscillation in the direction of the slip. The excited TTF-CA pairs may contribute to subsequent CT excitations of neighboring TTF-CA pairs as background charges. With these effects, the sequence of excited TTF-CA pairs is generated near the E structures.

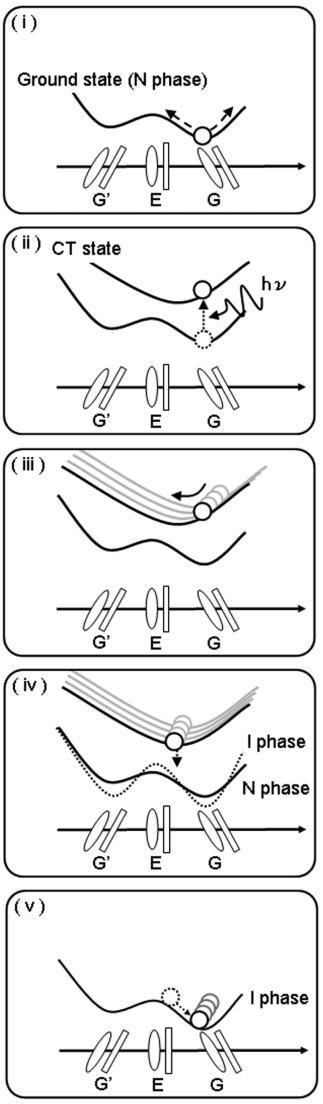

Figure 12. Conceptual potential energy curves of I and N phases along the slipping mode of TTF-CA pair in the initial process of N-to-I PIPT. Each ellipse stands for one TTF-CA pair.

(iv) The sequence of excited (dimerized) TTF-CA pairs falls into the potential energy surface of the I phase, which is not reproduced in a small number of dimerized TTF-CA pairs. The excited TTF-CA pair at the E structure is supposed to be suitable for the generation of the sequence of TTF-CA pairs in coherent motion because of the large charge bias between TTF and CA molecules and the long lifetime of CT excitation.

(v) According to the experimental data, the optimal structure of the I phase is supposed to be a dimerized G-like structure. For the sufficiently long sequence of the dimerized pairs, the I phase is expected to be more stable than the N phase. Otherwise, the N phase is expected to be so stable that the sequence of the dimerized pairs is broken. At high temperature, a thermal vibration hinders the generation of the sequence to make the N phase more stable.

The double-laser experiment[13] has given further information about the characteristic of N-to-I PIPT: The maximum ratio of photogenerated I phase is determined by the sum of the excitation density of two laser pulses and the reflectance change decays on the ps time scale, while there exists the oscillation of reflectance (the period T = 0.62 ps), which is nonlinear to the excitation density. The oscillation can be controlled by the delay time of two lasers: with delay time $\Delta t = T$, the oscillation is enhanced, while the oscillation disappears with Δt = 1.5 T. This oscillation can be explained with the environment change of neighboring TTF-CA pairs in process ii. This assumption is also consistent with the experimental attribution of reflectance oscillation in ref 12: the fast oscillation with the period of 0.62 ps is due to the lattice phonon corresponding to the dimeric molecular displacement, while the slow oscillation with about 50 ps is due to the shock wave.

The new mechanism explains the initial generation process of the I domain without collective excitation among several TTF-CA pairs. However, there remain several properties to be revealed in our mechanism: the electronic structure of the I phase, the crossing of the I and N PESs, and the multipair PESs with steric effects. The clear description of the I phase requires the excited state calculation of a dispersion-controlled solid state, which is costly and still challenging. For the rigorous discussion, better models containing stacked pairs would also be required. To perform such calculations, we need further computer power and theoretical development.

IV. CONCLUSION

In this study, we have carried out the excited state calculations of TTF-CA molecular crystal to clarify the initial neutral (N) to ionic (I) process of the photoinduced phase transition (PIPT) mechanism. For this purpose, we have used the state-of-the-art long-range corrected time-dependent density functional theory combined with the local response dispersion method.

First, we calculated the excitation spectrum of an isolated TTF-CA pair and succeeded in reproducing an accurate spectrum, which clearly explains the nature of each excitation. We next calculated the potential energy surfaces (PES) of the ground and lowest charge transfer (CT) excitations to make sure of the structural effect on the PIPT. As a result, we found that the ground state has a double minima on the PES and the CT state has a single minimum on the center of the double minimum as for the relative position change in a TTF-CA pair. On the basis of these results, we propose that the PIPT proceeds through the angle change of molecular planes.

To investigate the PIPT of TTF-CA crystal, we adopted an embedded TTF-CA pair in the background point charges for modeling TTF-CA crystal. Consequently, we found that the point charges of surrounding excited TTF-CA pairs obviously decrease the CT excitation energy of the TTF-CA pair and make the CT energy close to the experimental absorption energy (0.9 eV) through the angle change of the molecular planes. These point charges also increase the oscillator strength of this excitation. We therefore suggest that the CT excitation of the TTF-CA pair itself may contribute to the CT excitations of other neighboring TTF-CA pairs.

In summary, we propose that the PIPT of TTF-CA crystal proceeds as follows:

(i) In the ground state of the TTF-CA crystal, the molecular plane angles vary around the G structure by the thermal vibration.

(ii) By laser irradiation, the TTF-CA crystal is excited to the CT state. The electrostatic effect of the excited pair enhances the excitation of neighboring TTF-CA pairs. Thus, the sequence of excited TTF-CA pairs is generated in the *a* direction of TTF-CA (Figure 1).
(iii) The sequence of excited TTF-CA pairs transforms into the parallelistic (E) structure on the single minimum PES in the coherent motion.
(iv) The sequence of excited TTF-CA pairs is relaxed to the I phase surface, which is not realized in one TTF-CA pair.
(v) The generated I phase domain varies to the optimal structure. In the N-to-I PIPT, where the temperature is high, the stability of the I phase is insufficient and the thermal vibration breaks the unstable I phase into the N phase.

AUTHOR INFORMATION

Corresponding Author
*E-mail: tsuneda@riken.jp.

ACKNOWLEDGMENT

This research was supported by the Japanese Ministry of Education, Culture, Sports, Science and Technology (MEXT) (Grants: 20350002 and 20038012). The numerical calculations were conducted on the RIKEN Cluster of Clusters (RICC). One of the authors (T.T.) would like to thank Canon Inc. and Hitachi Chemical Co. Ltd. for their contributions.

REFERENCES

(1) Mayerle, J. J.; Torrance, J. B.; Crowley, J. I. *Acta Crystallogr. B* **1979**, *35*, 2988–2995.
(2) Torrance, J. B.; Vazquez, J. E.; Mayerle, J. J.; Lee, V. Y. *Phys. Rev. Lett.* **1981**, *46*, 253–257.
(3) Torrance, J. B.; Girlando, A.; Mayerle, J. J.; Crowley, J. I.; Lee, V. Y.; Batail, P.; LaPlaca, S. J. *Phys. Rev. Lett.* **1981**, *47*, 1747–1750.
(4) Le Cointe, M.; Lemée-Cailleau, M. H.; Cailleau, H.; Toudic, B.; Toupet, L.; Heger, G.; Moussa, F.; Schweiss, P.; Kraft, K. H.; Karl, N. *Phys. Rev. B* **1995**, *51*, 3374–3386.
(5) Girlando, A.; Marzola, F.; Pecile, C.; Torrance, J. B. *J. Chem. Phys.* **1983**, *79*, 1075–1085.
(6) Koshihara, S.; Tokura, Y.; Mitani, T.; Saito, G.; Koda, T. *Phys. Rev. B* **1990**, *42*, 6853–6856.
(7) Luty, T.; Cailleau, H.; Koshihara, S.; Collet, E.; Takesada, M.; Lemée-Cailleau, M. H.; Buron-Le Cointe, M.; Nagaosa, N.; Tokura, Y.; Zienkiewicz, E.; Ouladdiaf, B. *Europhys. Lett.* **2002**, *59*, 619–625.
(8) Guérin, L.; Collet, E.; Lemée-Cailleau, M. H.; Buron-Le Cointe, M.; Cailleau, H.; Plech, A.; Wulff, M.; Koshihara, S.; Luty, T. *Chem. Phys.* **2004**, *299*, 163–170.
(9) Iwai, S.; Tanaka, S.; Fujimura, K.; Kishida, H.; Okamoto, H.; Tokura, Y. *Phys. Rev. Lett.* **2002**, *88*, 057402.
(10) Tanimura, K. *Phys. Rev. B* **2004**, *70*, 144112.
(11) Collet, E.; Lemée-Cailleau, M. H.; Buron-Le Cointe, M.; Cailleau, H.; Wulff, M.; Luty, T.; Koshihara, S.; Meyer, M.; Toupet, L.; Rabiller, P.; Techert, S. *Science* **2003**, *300*, 612–615.
(12) Okamoto, H.; Ishige, Y.; Tanaka, S.; Kishida, H.; Iwai, S.; Tokura, Y. *Phys. Rev. B* **2004**, *70*, 165202.
(13) Iwai, S.; Ishige, Y.; Tanaka, S.; Okimoto, Y.; Tokura, Y.; Okamoto, H. *Phys. Rev. Lett.* **2006**, *96*, 057403.
(14) Messerschmidt, M.; Tschentscher, T.; Cammarata, M.; Meents, A.; Sager, C.; Davaasambuu, J.; Busse, G.; Techert, S. *J. Phys. Chem. A* **2010**, *114*, 7677–7681.
(15) Uemura, H.; Okamoto, H. *Phys. Rev. Lett.* **2010**, *105*, 258302.
(16) Guérin, L.; Hébert, J.; Buron-Le Cointe, M.; Adachi, S.; Koshihara, S.; Cailleau, H.; Collet, E. *Phys. Rev. Lett.* **2010**, *105*, 246101.
(17) Metzger, R. M.; Torrance, J. B. *J. Am. Chem. Soc.* **1985**, *107*, 117–121.
(18) Kawamoto, T.; Iizuka-Sakano, T.; Shimoi, Y.; Abe, S. *Phys. Rev. B* **2001**, *64*, 205107.
(19) Soos, Z. G.; Kuwajima, S.; Harding, R. H. *J. Chem. Phys.* **1986**, *85*, 601–610.
(20) Nagaosa, N.; Ogawa, T. *Phys. Rev. B* **1989**, *39*, 4472–4483.
(21) Huai, P.; Zheng, H.; Nasu, K. *J. Phys. Soc. Jpn.* **2000**, *69*, 1788–1800.
(22) Yonemitsu, K. *J. Phys. Soc. Jpn.* **2004**, *73*, 2868–2878.
(23) Yonemitsu, K. *J. Phys. Soc. Jpn.* **2004**, *73*, 2879–2886.
(24) Yonemitsu, K. *J. Phys. Soc. Jpn.* **2004**, *73*, 2887–2893.
(25) Yonemitsu, K.; Nasu, K. *Phys. Rep.* **2008**, *465*, 1–60.
(26) Oison, V.; Katan, C.; Rabiller, P.; Souhassou, M.; Koenig, C. *Phys. Rev. B* **2003**, *67*, 035120.
(27) Giovannetti, G.; Kumar, S.; Stroppa, A.; van den Brink, J.; Picozzi, S. *Phys. Rev. Lett.* **2009**, *103*, 266401.
(28) Ishibashi, S.; Terakura, K. *Phys. B* **2010**, *405*, S338–S340.
(29) Filatov, M. *Phys. Chem. Chem. Phys.* **2011**, *13*, 144–148.
(30) Tawada, Y.; Tsuneda, T.; Yanagisawa, S.; Yanai, T.; Hirao, K. *J. Chem. Phys.* **2004**, *120*, 8425–8433.
(31) Iikura, H.; Tsuneda, T.; Yanai, T.; Hirao, K. *J. Chem. Phys.* **2001**, *115*, 3540–3544.
(32) Tawada, Y.; Chiba, M.; Tsuneda, T.; Hirao, K. *J. Chem. Phys.* **2006**, *124*, 144106.
(33) Sato, T.; Nakai, H. *J. Chem. Phys.* **2009**, *131*, 224104.
(34) Song, J.-W.; Tsuneda, T.; Sato, T.; Hirao, K. *Org. Lett.* **2010**, *12*, 1440–1443.
(35) Seidl, A.; Görling, A.; Vogl, P.; Majewski, J. A.; Levy, M. *Phys. Rev. B* **1996**, *53*, 3764–3774.
(36) Becke, A. D. *Phys. Rev. A* **1988**, *38*, 3098–3100.
(37) Tsuneda, T.; Suzumura, T.; Hirao, K. *J. Chem. Phys.* **1999**, *110*, 10664–10678.
(38) Hehre, W. J.; Ditchfield, R.; Pople, J. A. *J. Chem. Phys.* **1972**, *56*, 2257–2261.
(39) Hariharan, P. C.; Pople, J. A. *Theor. Chim. Acta* **1973**, *28*, 213–222.
(40) Francl, M. M.; Petro, W. J.; Hehre, W. J.; Binkley, J. S.; Gordon, M. S.; DeFrees, D. J.; Pople, J. A. *J. Chem. Phys.* **1982**, *77*, 3654–3665.
(41) Frisch, M. J.; Trucks, G. W.; Schlegel, H. B.; Scuseria, G. E.; Robb, M. A.; Cheeseman, J. R.; Montgomery, J. A., Jr.; Vreven, T.; Kudin, K. N.; Burant, J. C.; Millam, J. M.; Iyengar, S. S.; Tomasi, J.; Barone, V.; Mennucci, B.; Cossi, M.; Scalmani, G.; Rega, N.; Petersson, G. A.; Nakatsuji, H.; Hada, M.; Ehara, M.; Toyota, K.; Fukuda, R.; Hasegawa, J.; Ishida, M.; Nakajima, T.; Honda, Y.; Kitao, O.; Nakai, H.; Klene, M.; Li, X.; Knox, J. E.; Hratchian, H. P.; Cross, J. B.; Bakken, V.; Adamo, C.; Jaramillo, J.; Gomperts, R.; Stratmann, R. E.; Yazyev, O.; Austin, A. J.; Cammi, R.; Pomelli, C.; Ochterski, J. W.; Ayala, P. Y.; Morokuma, K.; Voth, G. A.; Salvador, P.; Dannenberg, J. J.; Zakrzewski, V. G.; Dapprich, S.; Daniels, A. D.; Strain, M. C.; Farkas, O.; Malick, D. K.; Rabuck, A. D.; Raghavachari, K.; Foresman, J. B.; Ortiz, J. V.; Cui, Q.; Baboul, A. G.; Clifford, S.; Cioslowski, J.; Stefanov, B. B.; Liu, G.; Liashenko, A.; Piskorz, P.; Komaromi, I.; Martin, R. L.; Fox, D. J.; Keith, T.; Al-Laham, M. A.; Peng, C. Y.; Nanayakkara, A.; Challacombe, M.; Gill, P. M. W.; Johnson, B.; Chen, W.; Wong, M. W.; Gonzalez, C.; Pople, J. A. *Gaussian 03, Revision D.02*; Gaussian, Inc.: Wallingford, CT, 2004.
(42) Torrance, J. B.; Scott, B. A.; Welber, B.; Kaufman, F. B.; Seiden, P. E. *Phys. Rev. B* **1979**, *19*, 730–741.
(43) Andre, J. J.; Weill, G. *Mol. Phys.* **1968**, *15*, 97–99.
(44) Krishnan, R.; Binkley, J. S.; Seeger, R.; Pople, J. A. *J. Chem. Phys.* **1980**, *72*, 650–654.
(45) McLean, A. D.; Chandler, G. S. *J. Chem. Phys.* **1980**, *72*, 5639–5648.
(46) Blaudeau, J.-P.; McGrath, M. P.; Curtiss, L. A.; Radom, L. *J. Chem. Phys.* **1997**, *107*, 5016–5021.
(47) Jacobsen, C. S.; Torrance, J. B. *J. Chem. Phys.* **1982**, *78*, 112–115.
(48) Koshihara, S.; Takahashi, Y.; Sakai, H.; Tokura, Y.; Luty, T. *J. Phys. Chem. B* **1999**, *103*, 2592–2600.